Optics Communications 282 (2009) 2270–2277

Contents lists available at ScienceDirect

Optics Communications

journal homepage: www.elsevier.com/locate/optcom

Damped low-frequency surface-plasmon resonance in metal–dielectric periodic structures of planar semi-infinite extent

Hyoung-In Lee *

Optics and Photonics Elite Research Academy (OPERA), School of Information and Communication Engineering, Inha University, Incheon 402-751, Republic of Korea

ARTICLE INFO

Article history:
Received 25 July 2008
Received in revised form 17 February 2009
Accepted 20 February 2009

PACS:
41.20.Jb
42.70.Qs
73.20.Mf
78.67.−n

Keywords:
Nanophotonics
Surface-plasmon resonance
Periodic structure
Frequency limit
Wave propagation

ABSTRACT

In the low-frequency limit with respect to the bulk plasma frequency of metal, damped surface-plasmon resonance is examined for a periodic semi-infinite structure with metal–dielectric unit cells in slab geometry. In comparison to the author's earlier results in [1], the additional material damping is found to alter the resonance characteristics in many nontrivial ways. In particular, the damped Bloch waves propagating in the direction normal to the slab planes are induced, thereby altering wave stability with respect to the ratio of dielectric constants.

1. Introduction

As regards photonic periodic structures, the basic theory set forth in [2] dealt with the dielectric–dielectric (D–D) bilayer unit cells among other geometries. Periodic structures with unit cells composed of metal–dielectric (M–D) bilayers have attracted more attention from the nanophotonics community, since they had been thoroughly analyzed in [3]. Periodic structures are also examined as regards negative refraction and/or metamaterials, for instance, in [4]. It is now well-known that the enhanced transmission through such periodic M–D structures is related to the resonant tunneling due to the surface-plasmon resonances (SPRs) and the structural periodicity [2,3].

Along this line of approach, undamped surface-plasmon resonance was examined in [1] for a periodic semi-infinite structure with metal–dielectric unit cells in slab geometry as shown in Fig. 1. The importance of the Bloch factor denoting the quasi-periodicity in the out-of-plane depthwise direction (i.e., the $\tilde{x}$-direction in Fig. 1) has been rediscovered, in assessing the wave stability with respect to the ratio between two participating dielectric constants. The main finding in [1] was that wave stability increases as this ratio differs away from unity. However, the reason of publishing a new research paper of [1] for the geometry in Fig. 1 lies in investigating what happens in the low-frequency limit (LFL) with respect to the bulk plasma frequency of metal. Here in this paper, the material damping is introduced to see how the energy flow direction is altered in association with the complex Bloch factor [5]. The other interesting range of frequency just below the metal's plasma frequency was called the high-frequency limit (HFL) in [5], where SPRs have been investigated both with and without material damping for the same structure as in Fig. 1. Hence, Ref. [5] is the HFL counterpart of the LFL combination of Ref. [1] and the present paper. The results in the LFL and HFL are not entirely symmetric, thereby exhibiting a different dependence on the period. In particular, the effects of resonant tunneling [3] turn out more uniform in the present LFL, in comparison to more complex ones in the HFL [5].

This paper is organized as follows. In Section 2, the dispersion relation is derived for SPRs in the presence of material damping, and its reduction to the low-frequency limit is briefly discussed. In Section 3, the issue of wave stability is reviewed. In Section 4, complex solutions to the dispersion relation are discussed. In Section 5, various characteristics of frequency dispersion are explored on the iso-frequency contours. In Section 6, the Bloch angles are discussed as regards energy defocusing. In addition, the migrations

* Tel.: +82 32 860 8868; fax: +82 865 8845.
E-mail address: hileesam@naver.com

0030-4018/$ - see front matter © 2009 Elsevier B.V. All rights reserved.
doi:10.1016/j.optcom.2009.02.058

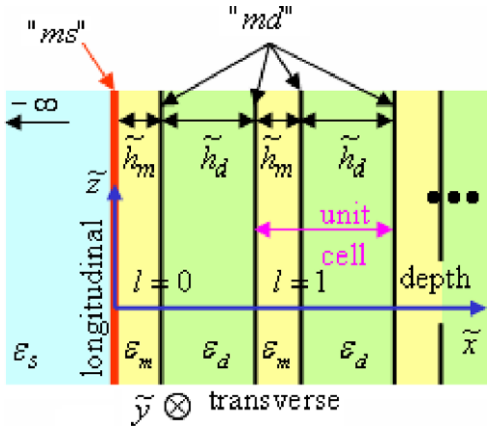

Fig. 1. Periodic semi-infinite structures.

of the complex roots are under examination with the variation in material damping. In Section 7, discussions are provided, and conclusions are drawn.

2. Problem formulation

Most of the notations follow those in [1], except for those employed in [5]. Except for the obvious cases, dimensional quantities are denoted by overhead tilde signs, while dimensionless ones are without tildes. The terms lossy and lossless will be used interchangeably with "with" and "without" material damping, respectively. Table 1 lists key parameters and variables as an occasional reminder. The plasma frequency and light speed in vacuum are denoted by $\tilde{\omega}_p$ and $\tilde{c}_0$, respectively. Correspondingly, the plasma wave number $\tilde{k}_p = \tilde{\omega}_p/\tilde{c}_0$ and plasma wavelength $\lambda_p = 2\pi\tilde{c}_0/\tilde{\omega}_p$ are defined. In consideration of Fig. 1, the time $\tilde{t}$ and space coordinates $(\tilde{x}, \tilde{y}, \tilde{z})$ in the depthwise, longitudinal, and transverse directions are made dimensionless such that $\tau = \tilde{\omega}_p\tilde{t}$ and $(X, Y, Z) = \tilde{k}_p(\tilde{x}, \tilde{y}, \tilde{z})$. A unit cell is composed of one metallic sub-layer and its adjacent dielectric sub-layer of the respective thicknesses $\tilde{h}_m$ and $\tilde{h}_d$. The dimensionless thicknesses are formed such that $h_j = \tilde{k}_p\tilde{h}_j$ with $j = m, d$. Hence, the period or unit-cell thickness is given by the sum $h_u = h_m + h_d$. In addition, the metal's filling fraction f is defined by $f = \tilde{h}_m/\tilde{h}_u$. The relative dielectric constants are denoted by ε_j, now with $j = m, d, s$. For the operating frequency $\tilde{\omega}$, the reduced frequency is defined by $\Omega = \tilde{\omega}/\tilde{\omega}_p$. The material dispersion of metal $\varepsilon_m = \varepsilon_{mr} - i\varepsilon_{mi}$ is given by the lossy Drude model $\varepsilon_m = 1 - [\tilde{\omega}(\tilde{\omega} - i\tilde{\gamma}_1)]^{-1}\tilde{\omega}_p^2$ with $i = (-1)^{1/2}$. Here, γ_1 is the material damping frequency [5–8]. In dimensionless form,

$$\varepsilon_m = 1 - \frac{1}{\Omega^2}\frac{1}{1 - i\gamma}, \quad \gamma = \frac{\tilde{\gamma}_1}{\tilde{\omega}} > 0 \tag{1}$$

As a consequence, the metallic nature $\varepsilon_{mr} < 0$ is ensured for $(1 + \gamma^2)\Omega^2 < 1$. It is noted that $\varepsilon_d, \varepsilon_s > 0$, where the subscript s implies the substrate. In particular, γ was conveniently introduced for Fig. 5 of [6]. For reference, the lossless Drude model is then defined to be $\varepsilon_m = 1 - \Omega^{-2}$ when setting $\gamma_1 = 0$ or $\gamma = 0$. For an numerical example with $(\Omega, \gamma) = (0.25, 0.0341)$, $\varepsilon_m = -15.0 - i0.545$ according to Eq. (1), which turn out not to be a bad approximation to $\varepsilon_m = -15.0 - i1.1$ shown in Fig. 1 of [7].

The transverse-magnetic (TM) waves are described by $\vec{E} = (E_x, 0, E_z)$ and $\vec{H} = (0, H_y, 0)$. Longitudinally propagating waves are represented by the factor $\exp\left[i(\tilde{\omega}\tilde{t} - \tilde{\beta}\tilde{z})\right]$, with the complex $\tilde{\beta}$ as the longitudinal propagation constant. The component H_y is then expressed by $H_y(\tau, X, Z) = F(X)\exp[i(\Omega\tau - bZ)]$, where $b = \tilde{\beta}/\tilde{k}_p = b_r - ib_i$. According to the phasor $\exp(i\Omega\tau)$, the factor $(1 - i\gamma)$ in Eq. (1) is chosen for ε_m, and therefore, $\varepsilon_{mi} > 0$ is compatible with $\gamma > 0$ [5]. Besides, the dimensionless parameters $D_j = (b^2 - \varepsilon_j\Omega^2)^{1/2}$ and $U_j = (\varepsilon_j\Omega)^{-1}D_j$ are introduced for TM waves. The profile in the 0 th unit cell is denoted by $F_j^0(X) = \sum_{\chi=\pm}A_{j\chi}\exp\left[\chi D_j(X - \delta_{dj}h_m)\right]$, where $A_{j\pm}$ are undetermined coefficients, and δ_{dj} is the Kronecker's symbol. It is noticed here that $F_m^0(X)$ and $F_d^0(X)$ are defined over the intervals $X \in [0, h_m]$ and $X \in [h_m, h_u]$, respectively. Its counterpart in the l th unit cell is then represented via the Bloch-Floquet theorem as follows [4,5]:

$$F_j^l(X) = \Gamma^l F_j^0(X - l\Delta_u), \quad \Gamma = |\Gamma|\exp(-i\mu) \tag{2}$$

For the Bloch factor Γ, its amplitude $|\Gamma|$ is the attenuation (or amplification) constant per unit cell, while the Bloch angle μ is the relative phase with increasing unit-cell number. In the meantime, the depthwise profile $F_s(X) = C_s\exp(D_sX)$ is assumed for the semi-infinitely extended medium lying in the domain $X < 0$, with C_s as an yet another undetermined coefficient. The following surface-wave condition (SWC) is necessary for evanescent waves to be supported in the substrate:

$$\Re(D_s) = \Re(\sqrt{b^2 - \varepsilon_s\Omega^2}) > 0 \tag{3}$$

Hence, the light line for the substrate is defined by the curve $\Re(D_s) = 0$ [1,5]. In other words, the wave-vector regime $|b| < \varepsilon_s^{1/2}\Omega$ for the volume (guided) waves reduces to null in the LFL $\Omega \to 0^+$. The dispersion relation valid for any Ω is obtained to be

$$2 + [(\Pi_+ - \Pi_-)\coth(D_dh_d) + (\Pi_+ + \Pi_-)]\tanh(D_mh_m) = 0 \tag{4}$$

Here, $\Pi_\pm = [U_m(U_s \pm U_d)]^{-1}[(U_m)^2 \pm U_sU_d]$. As is well-known, the transverse-electric (TE) waves do not support SPRs throughout the whole structure [1]. As an aside, it is remarked however that there are no surface waves but volume waves on the substrate side for TE waves [2].

With reference to Eq. (1), the low-frequency limit (LFL) is defined by the limit $\Omega \to 0^+$, in which $(-\varepsilon_{mr}) \to \infty$ [3,7]. A formal limiting procedure can be worked out on Eq. (4), in parallel with that in [1]. It is worth mentioning that the parameter $b_\gamma = \lim_{\Omega\to 0^+} D_m = [b^2 + (1 - i\gamma)^{-1}]^{1/2}$ appears in this process. There are now two kinds of the distinguished limits as follows:

$$W^2 = \varepsilon_d \lim_{\Omega f \to 0^+}\left(\frac{\Omega^2}{f}\right), \quad \gamma = \lim_{\Omega,\gamma_2\to 0^+}\frac{\gamma_2}{\Omega}. \tag{5}$$

In the first distinguished limit $f \to 0^+$ and $\Omega \to 0^+$ $(\Omega, f \to 0^+)$ of Eq. (5), Eq. (3.6) of [1] remains the same, but $\tanh(fh_ub_\gamma) \to fh_ub_\gamma$ for Eq. (4) in place of Eq. (3.7) of [1]. In the second distinguished limit of Eq. (5), another limit $\gamma_2 \to 0^+$ is now introduced for small material

Table 1
Key parameters and variables. Dimensional quantities are denoted by overhead tilde signs, while dimensionless ones are without tildes.

$X = \tilde{k}_p\tilde{x}, \tau = \tilde{\omega}_p\tilde{t}, \tilde{k}_p = \tilde{\omega}_p/\tilde{c}_0, \lambda_p = 2\pi\tilde{c}_0/\tilde{\omega}_p, h_j = \tilde{k}_p\tilde{h}_j, f = \tilde{h}_m/\tilde{h}_u, b = b_r - ib_i, b = \tilde{\beta}/\tilde{k}_p,$
$\Omega = \tilde{\omega}/\tilde{\omega}_p, \varepsilon_m = \varepsilon_{mr} - i\varepsilon_{mi}, \gamma = \tilde{\gamma}_1/\tilde{\omega}, \gamma_2 = \tilde{\gamma}_1/\tilde{\omega}_p, \gamma = \gamma_2/\Omega, D_j = \sqrt{b^2 - \varepsilon_j\Omega^2},$
$U_j = (\varepsilon_j\Omega)^{-1}D_j, \Gamma = \Gamma_r - i\Gamma_i, \Gamma = |\Gamma|\exp(-i\mu), b_m = b_\gamma = \sqrt{b^2 + (1 - i\gamma)^{-1}}, b_\gamma = b_{\gamma,r} - ib_{\gamma,i},$
$b_d = b, R = \varepsilon_s/\varepsilon_d, B = h_ub, V_p = \tilde{\omega}/(\tilde{c}_0\tilde{\beta}) = \Omega/b), V_g = \tilde{c}_0^{-1}(\partial\tilde{\omega}/\partial\tilde{\beta}) = \partial\Omega/\partial b, W^2 \sim \varepsilon_d(\Omega^2/f),$
$\Sigma_{f3} = \Sigma_W \cup \Sigma_\gamma \cup \Sigma_\Gamma, \Sigma_{a3} = \Sigma_B - \Sigma_{f3}$